REVISTA MATÉRIA V.27 N.04
ISSN 1517-7076 articles e20220181, 2022

On the mechanical properties and crack pattern analysis of a strain-hardening cement-based composite reinforced by natural sisal fibers

Felipe Pinheiro Teixeira[1], Felipe Rodrigues de Souza[2], Victor Nogueira Lima[2], Flávio de Andrade Silva[2], Sergio Luis González Garcia[1]

[1]Universidade Estadual do Norte Fluminense Darcy Ribeiro, Programa de Pós-Graduação em Engenharia Civil. Avenida Alberto Lamego, 2000, 28013-602, Campos dos Goytacazes, RJ, Brasil.

[2]Pontifícia Universidade Católica do Rio de Janeiro, Departamento de Engenharia Civil e Ambiental. Rua Marques de São Vicente, 225, 22451-900, Rio de Janeiro, RJ, Brasil.

e-mail: felipe.pinheiro.teixeira@gmail.com, felipe@arkko.com.br, eng.vnl@gmail.com, fsilva@puc-rio.br, liluiser@uenf.br

ABSTRACT

Besides the strength enhancement and strain improvement (strain-hardening behavior), the use of natural fibers as reinforcement in cement-based matrices can also be highlighted as an economical and eco-friendly alternative for the future of the construction industry. In the present work, cement-based composites reinforced by natural sisal fibers were produced and tested under direct tensile loading. The Portland cement was partially replaced by pozzolans (metakaolin – MK and fly ash – FA), aiming to produce a calcium hydroxide-free matrix to ensure the durability of the fibers. The natural sisal fibers were used in a 5% volume fraction (in mass), divided into three layers. The mechanical properties of composite plates were compared to other literature results and demonstrated to be compatible with recent research. The crack pattern was analyzed by Digital Image Correlation (DIC) for a better understanding of their failure mechanisms. The material presented a tensile strength increase after the first crack formation, marked by multiple cracking partners from this point. Finally, a comparison between direct (LVDTs) and indirect (DIC) methods of strain measurement was done and demonstrated minor results for the DIC, approximately 84% of those obtained from the LVDTs.

Keywords: Cement composite; Natural fibers; Mechanical properties; Crack pattern analysis.

1. INTRODUCTION

As a substitution for the synthetic, metallic and glass fibers in cement matrices, natural fibers appear as an eco-friendly alternative capable to provide the desired mechanical properties with the benefit of reducing costs and CO_2 emissions. Recently, natural plant fibers, such as sisal, jute, hemp, cotton, coir, bamboo and curaua have been considered as possible sustainable substituent fibers [1–6].

The use of natural fibers in cementitious matrix composites can considerably improve the physical-mechanical properties of the material [4, 5, 7–9], can significantly reduce the material cost [10, 11], and can reduce the environmental impact caused by the production process of the mixing materials [12]. Consequently, several configurations of natural fibers have been mechanically explored in cement-based composites, such as the textile form [13–15], short and randomly dispersed in the matrix [16–18], or in a continuous and aligned way [19–21]. Despite the benefits cited, natural fibers have a high ability to absorb moisture [22] and may develop durability problems when in the alkaline environment of the cement matrix [1, 23].

The hydrophilic nature of these fibers results in a high moisture absorption capacity, which can absorb part of the matrix water and increase the fiber dimension. This mechanism may lead to an interface weakening [24] and the decrease of the water-cement ratio of the matrix [16]. To avoid it, the fibers' pre-saturation can be a solution, as the saturated fibers can act as a water repository, leading to delayed hydration of the non-hydrated cement grains, increasing the strength and density of the interface [22]. According to Silva Junior et al. [25], the composites with saturated fibers showed smaller crack width, higher toughness, and higher tensile strength when compared to those with natural humidity fibers.

To ensure the natural fibers durability in the cement matrices' alkaline environment, it is necessary to prevent alkaline degradation and mineralization [1, 23]. For such, the pozzolanic additions to precipitate the calcium hydroxide of the matrix as calcium silicate hydrate can eliminate the degradation risks and improve the

Corresponding Author: Felipe Pinheiro Teixeira Received on 20/07/2022 Accepted on 12/09/2022

DOI: https://doi.org/10.1590/1517-7076-RMAT-2022-0181

durability of this kind of composite [26]. FERREIRA *et al*. [27, 28] presented a Portland cement replacement by metakaolin (30%) and fly ash (40%) for their sisal fibers cement composites. The authors justify that such alteration provided a calcium hydroxide free matrix and, consequently, the higher fibers durability. WEI and MEYER [29] showed by thermogravimetric analyses that the metakaolin and nano-clay addition significantly reduced the calcium hydroxide and the ettringite formation. Another positive effect of the Portland cement partially replacement by metakaolin and nano-clay was the fiber-matrix adhesion, resulting in a pullout energy 131% and 196% higher than reference samples.

As stated above, natural fibers can be randomly dispersed or even can be placed as a continuous and aligned reinforcement. CASTOLDI *et al*. [30] investigated the mechanical behavior of concretes reinforced with discrete fibers of polypropylene and sisal with the same length (51 mm) and considering different dosages (3, 6 and 10 kg/m^3). The composites were tested under monotonic and cyclic three-point bending loads, and they stated that sisal fiber can provide the same level of residual strength as polypropylene fiber, provided that the equivalence of fiber strengths is considered.

On the other hand, continuous fiber-reinforced cement composites can be considered high-performance construction materials due to their superior tensile strength and ductility [19, 25, 31, 32]. The improved mechanical properties and its considerable strength make this kind of material suitable for use as structural panels, impact and blast resistance, repair, and retrofit applications [33]. The behavior of these composites during tensile tests is characterized by multiple transverse cracks, which appear along its length as the loading increase. In this cracking process, the material toughness, strength, and strain capacity are directly associated with the fibers' properties, the cement matrix, and the interfacial bond and anchorage between them [34–36].

The interfacial bond and the anchorage between fiber and matrix govern the mechanical properties of the composite in the post-cracking regime [37–41]. However, it should be noted that a significantly strong bond between fiber and matrix does not guarantee the ductility of the material by itself, since in addition to the quality of the interface, the quality of the fiber and matrix individually must be considered. Therefore, fiber tensile strength, matrix microstructure, and fiber length, alignment, and content are important to the process of mitigating crack propagation [42]. Furthermore, in the case of composites with aligned fibers, attention should be paid to the number of reinforcement layers, the distance between them, and the thickness and quality of the matrix covering layer, in order to enhance the fiber's action in controlling the opening of cracks [32, 43].

Depending on the fiber content and on the interface between fiber and matrix, if the fiber volume is sufficient, the cementitious composite will not present a brittle failure after the first crack formation. In this case, the ductility will be enhanced, and the strain capacity will be significantly improved as the load increases. After the first crack, several other cracks are formed, and the failure will be marked by the fibers' pull-out. Also, considerable energy dissipation can be noticed [44–46].

The strain-hardening behavior can also be described by four distinct stages of the stress-strain curve [31, 47, 48]: Stage I corresponds to the linear-elastic range where both matrix and fiber behave linearly, which ends by the first crack formation when the bend over point – BOP is reached (the start of the first crack (BOP–) to its end (BOP+), after its propagation across the specimen's width); Stage II exhibits a stiffness decreases due to the formation of distributed cracks at regular intervals and, after the total amount of cracks is done, the progressive debonding takes place to the fibers' pullout at Stage III; finally, the post-peak response occurs in Stage IV, which only presents the residual strength (softening branch).

Although several studies have already addressed the basic properties of fiber-aligned cement-based composites, this paper explores the analysis of the crack pattern using the digital image correlation technique, comparing the results with research available in the literature, and the comparison between different methods of external deformation acquisition. Therefore, this work seeks to fill the gap of mechanically analyzing the composite and evaluating the test setup outputs.

2. MATERIALS AND METHODS

2.1. Sisal fibers

The sisal fibers used in this work were provided by the Community Association for the Production and Commercialization of Sisal – APAEB, located in Valente city, in the state of Bahia – Brazil. The fibers extraction from the *Agave sisalana* plant was done by decortication process [4, 49]. The fibers were received in bundles, measuring approximately one meter in length, and were manually brushed to detangle them. Different from the other authors that also used natural fibers [30, 32, 43, 50], the sisal fibers were not washed in warm water. In this experiment, just brushing and cutting in the demanded length were executed. Some mechanical and morphological characteristics of sisal fibers are summarized in Table 1.

Table 1: Summarized mechanical and morphological characteristics of sisal fibers [30, 50–52].

MECHANICAL	Tensile strength (MPa)	357 to 484
	Strain to failure (%)	3.3 to 14.7
	Modulus (GPa)	8.7 to 19.5
MORPHOLOGICAL	Fiber cross section area (mm^2)	0.02 to 0.03
	Microfibers per cross section (unit)	144 to 228
	Cell wall thickness (µm)	2.60 to 2.95

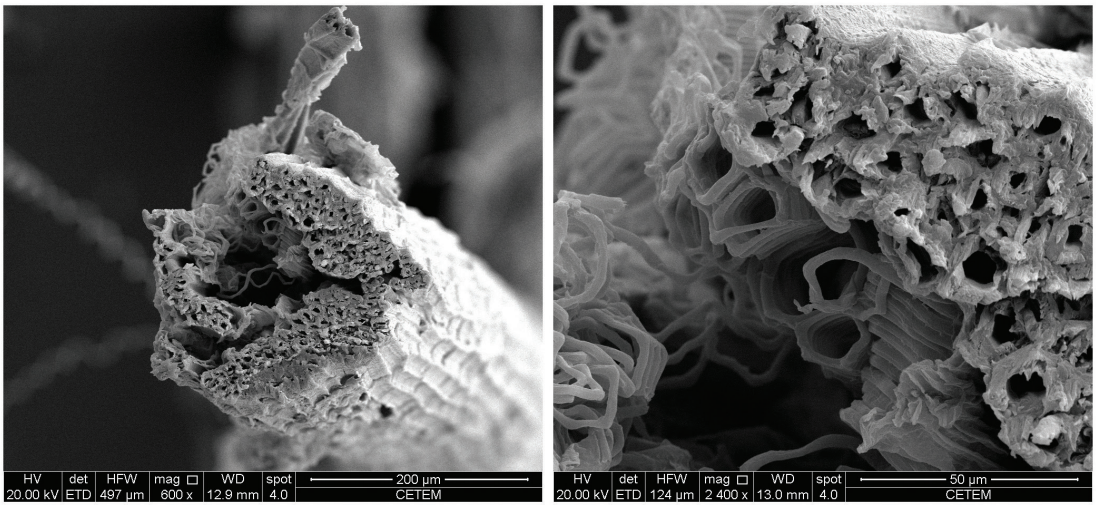

Figure 1: The sisal fiber cross-section images, in which is possible to see its rough longitudinal surface (a), the lumens and the microfibrils (b).

On the natural fibers structural view [51, 52], it is summarily composed of a bundle of microfibers in an aligned arrangement. Each microfiber is formed by a layered structure, named cell walls, composed of a primary wall and three secondary walls. These cell walls are made by microfibrils, which are disorderly arranged in the primary wall (like a mesh) and following a helical shape in the secondary walls. Another microfibers characteristic is the hollow that makes it looks like a tube, called the lumen. Figure 1 shows a cross-section of the used sisal fiber (Figure 1a) and its magnification (Figure 1b), both by a Scanning Electron Microscope (SEM) model FEI Quanta 400 (Thermo Fisher Scientific, Hillsboro, OR, USA).

2.2. Matrix desing

The cement matrix was designed for the 1:1:0.4 ratio (cementitious content, sand, and water). The cementitious content was made of 50% Portland cement type CPV, according to Brazilian standard NBR 16697 [53]; 40% metakaolin (MK), from BASF in Germany; and 10% fly ash (FA), from POZOFLY. The supplementation by pozzolans (MK and FA) aims to produce a calcium hydroxide-free matrix, providing an unaggressive environment for the natural fibers, as previously reported [5]. The quartz sand adopted presents a maximum diameter of 1.18 mm and 2.67 g/cm^3 of density. The GLENIUM® 3500 superplasticizer was used in a proportion of 2% of the cementitious content, in mass, to offer the required workability. The matrix presented compressive strength equal to 80.1 ± 4.4 MPa after 28 days. Seven cylindrical specimens measuring 100 mm in height and 25 mm in radius were used in the compression tests.

2.3. Manufacturing

For the matrix homogenization, the cementitious content, the quartz sand, and a portion of the water were mixed in a bench-mounted planetary blender; after this, the superplasticizer was diluted in the remaining water and slowly spilled down into the running mixer. Seeking to minimize the water absorption from the matrix by the porous fiber structure and provide better workability, the sisal fibers were submerged in water for one hour to reach their maximum saturation [34]. After saturation, the fibers were air-dried for 15 minutes to eliminate the extra humidity on their surface.

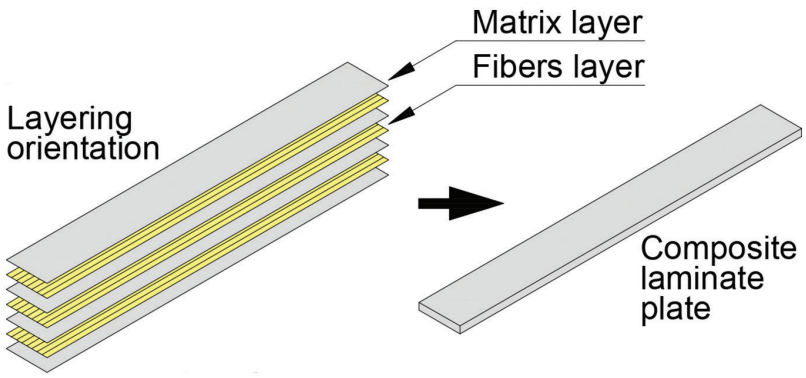

Figure 2: Layering schematic illustration.

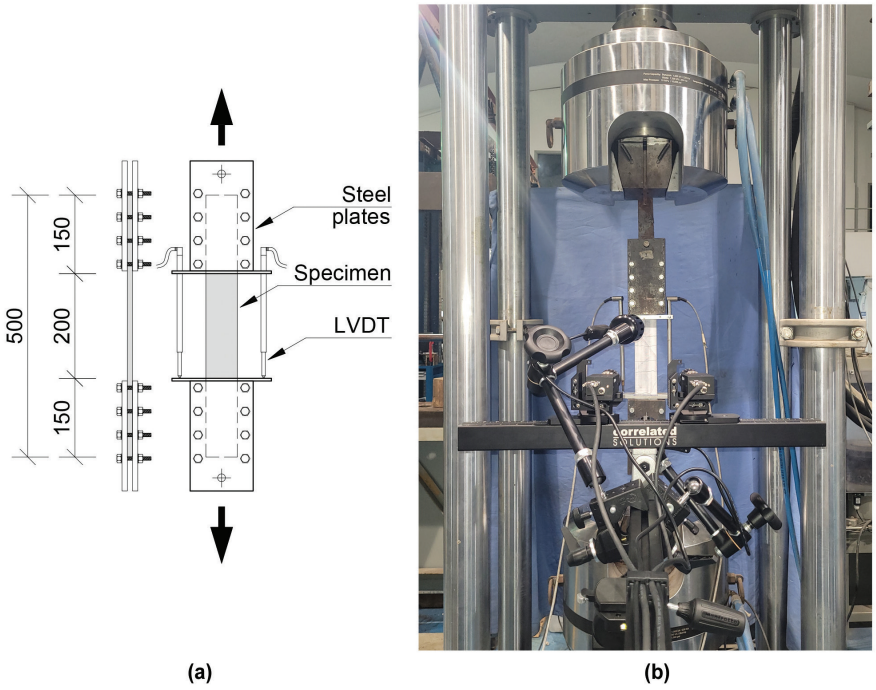

Figure 3: The schematic parameters of tensile tests with dimensions in mm (a) and the cameras setup during the tests (b).

For the composite manufacturing process, a matrix layer was placed in steel molds followed by a layer of sisal fibers, one layer at a time. The sisal fibers amount per specimen corresponds to a volume fraction of 5%, divided into three layers. It is worth mentioning that sisal fibers were longitudinally oriented, continuously, and without overlaps. The laminate composite plates presented 500 mm length, 60 mm width, and 10 mm thickness. Figure 2 presents a schematic illustration of the layering orientation.

2.4. Tensile tests

The tensile loading on composite plates was performed in a servo-hydraulic MTS 311 system with a 1000 kN load cell and a pair of external LVDTs (MTS, Eden Prairie, MN, USA). The specimens were fixed in steel plates with clamped screws controlled by a torque (8.5 Nm), and the tests were carried on under displacement control at a 0.1 mm/min rate. For this work, seven specimens were tested up to failure. Figure 3a presents a schematic about test parameters.

The cracking behavior were analyzed by Digital Image Correlation (DIC), a method capable of quantifying full-field deformations without physical contact [54, 55]. To proceed with this analysis, it was necessary to create a speckle pattern on the specimen's surface, which in this case, was made with a standardized paint roller used to produce random black dots over a white background. The process utilized two high-resolution digital cameras, model GS3-U351S5M by Point Grey, equipped with AF-X M100 Pro D lenses to monitor the specimen surface at a spatial resolution about 120 μm/pixel. The image acquisition was controlled by the Correlated

Table 2: Summarized mechanical properties.

SPECIMEN	FIRST-CRACK TENSILE STRENGTH (MPa)	ULTIMATE TENSILE STRENGTH (MPa)	STRAIN-TO-FAILURE (%)	YOUNG'S MODULUS (GPa)
SPEC 1	4.8	13.9	1.6	11.0
SPEC 2	4.5	9.9	1.0	23.0
SPEC 3	3.2	10.7	1.4	17.6
SPEC 4	3.2	10.8	1.6	17.9
SPEC 5	4.2	12.2	1.6	23.8
SPEC 6	3.4	12.3	1.8	11.2
SPEC 7	4.3	14.0	1.9	27.8
Mean ± SD	3.9 ± 0.6	12.0 ± 1.5	1.6 ± 0.3	18.8 ± 5.8

Solution's Vic-Snap 9 software in a 2 Hz capture frequency. The main goal of the imaging system is to use the images to calculate the specimen's deformations and strains over the test. For the DIC analyses, the Correlated Solution's Vic-3D 9 software were used, and the algorithm applied used the Gaussian weights over 47 pixels windows and one measured every 5 pixels to calculate the deformations and the strains. It is important to mention that only three specimens were submitted to this process. Figure 3b shows the camera setup during the tests.

3. RESULTS AND DISCUSSIONS

As expected, all the composite plates presented a strain-hardening performance with multiple cracks formation along their length. The stress-strain initial response was marked by a range of linear-elastic behavior up to the first crack appearance (stage I), and from this point, the load-carrying capacity remains increasing due to multiple cracking caused by the fibers bridging effect (stage II). These cracks were arranged at regular intervals and started to open exponentially when the new fissures stopped to appear, leading the composites up to their maximum stress (stage III). Thereafter, the crack-opening remains while load capacity slowly reduces (stage IV). Figure 4a present the mechanical behavior of all seven specimens tested while Figure 4b illustrates the different stages during the strain-hardening performance. The cement-based composite reinforced by sisal fibers reached a maximum tensile strength equal to 12.0 MPa at a strain capacity of 1.6% and modulus of 18.8 GPa, the first crack formation appeared at 3.9 MPa. Table 2 summarizes the composite mechanical properties.

For comparison, the composite mechanical behavior in the present work was confronted by the results of other authors [19, 25, 31, 32] who also used natural fibers in cement matrices. All these authors used the same specimen geometry adopted in the present work, except for thickness which varies according to the parameters such as the number of fiber layers, fibers volume, and manufacturing technique. The matrices were also very similar in composition, reinforced by sisal or curauá natural fibers. The fiber volume fraction adopted by the authors corresponded to 4% up to 10%, arranged in layers that vary between 1 to 5. Table 3 present the physical characteristics and mechanical comparison of all composite plates. The composites with three fiber layers presented similar strengths results, from 9.7 MPa up to 12.8 MPa. The specimen reinforced by a single layer showed significant strength decrease (47.5% lower) while the five layers specimen exhibited a substantial increase (22.5% higher), both compared to the composite in the present work. Though it is known that the fiber volume increase is directly associated with the strain-hardening capacity, in this comparison, it is not possible to verify a precise relation between strength and fiber volumetric fraction above 5%. For example, the high-performance composite presented by SILVA *et al*. [31] (10% of volume) showed the same maximum strength as the composite produced in the present work (5% of volume), both reinforced with the same type of natural fiber (sisal). Furthermore, SILVA JUNIOR *et al*. [25] used a volumetric fraction equal to 6% in composites reinforced by curauá fibers and reached 10.2 MPa, 15% lower than the achievement in the present work. However, it is worth mentioning that the composite by SOUZA *et al*. [19], with 8.5% volume (curauá fibers), presented the highest strength among all. In general, the authors describe a similar strain capacity at failure, except for TEIXEIRA and SILVA [32] and their three layers curauá composite, which exhibited a strain result 68.8% higher than specimens presented in this work.

Through DIC analysis, it was possible to generate a strain map (SPEC 5 specimen), which presents the strain fields (ε_{yy}) concerning the orientation of the tensile test (Y-axis). As the stress increases, transverse cracks gradually appear along the specimen length, one after another. At the maximum number of cracks is reached (end of stage II), the cracks start to open, bridged by the fibers (causing fibers to stretch and begin to split, up

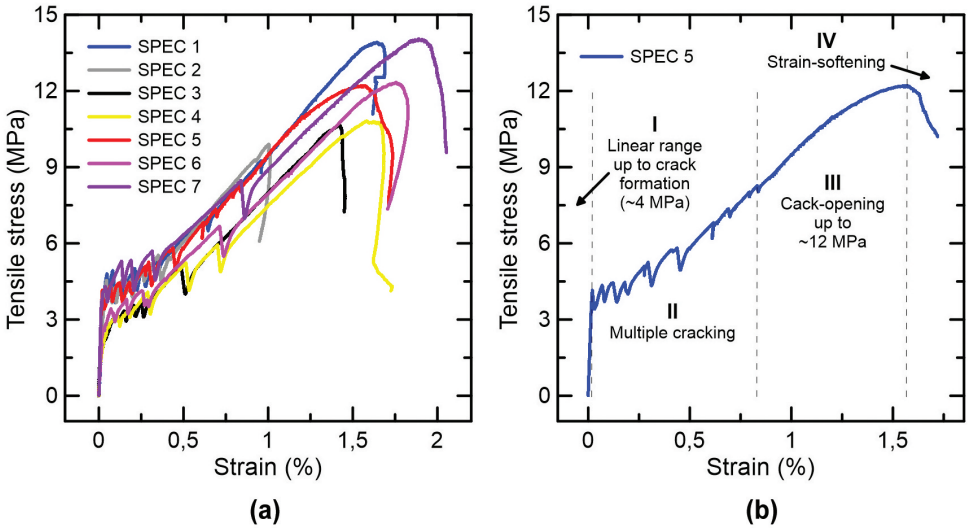

Figure 4: Mechanical behavior of all seven specimens (a) and the described stages of strain-hardening performance (b).

Table 3: Comparative of mechanical properties under tensile tests.

REFERENCES	NATURAL FIBERS BASE (kind)	NUMBER OF FIBER LAYERS (unity)	FIBER VOLUME FRACTION (%)	ULTIMATE TENSILE STRENGTH (MPa)	ULTIMATE TENSILE STRENGTH VARIATION (%)	STRAIN-TO-FAILURE mm/mm	STRAIN VARIATION (%)
Present work	Sisal	3	5.0	12.0	–	0.016	–
SILVA *et al*. [31]	Sisal	5	10.0	12.0	0	0.015	6.3 (lower)
SOUZA *et al*. [19]	Curauá	1	4.0	6.3	47.5 (lower)	0.012	25.0 (lower)
	Curauá	3	7.0	9.7	19.2 (lower)	0.014	12.5 (lower)
	Curauá	5	8.5	14.7	22.5 (higher)	0.016	0
TEIXEIRA and SILVA [32]	Curauá	3	5.0	12.8	6.7 (higher)	0.027	68.8 (higher)
SILVA JUNIOR *et al*. [25]	Sisal	3	6.0	10.2	15.0 (lower)	0.015	6.3 (lower)

to the end of stage III). These mechanisms are responsible for the post-crack stiffness increase presented by the composite, and its progression is graphically described by strain distribution along the longitudinal Y-axis at each stage in Figure 5. At the end of stage I, just a single crack is formed (represented by a peak), while at the end of stage II several cracks are already disseminated along with the specimen; and finally, at the end of stage III, the established cracks present a distinct evolution. As mentioned by YAO *et al*. [56], by the correlation of the strain fields with the strain distribution along the longitudinal Y-axis, it is possible to identify three different zones intrinsic to the cracking pattern of this kind of composite: a) the localization zones, in red, in which the cracks present the higher image strain and load is majority carried by the fibers; b) the shear lag zones, in blue and green, marked by the bond tensions between the fibers and the cement matrix (this zone precedes the crack appearance and remains adjacent after its establishment); and c) the uniform zones, where there isn't any crack formed and the composite still presenting a linear behavior.

The DIC analyses also provided the number of cracks established, their opening range, and the average spacing between then; these parameters are described in Table 4. The measurements were observed at the end of stage III when the composites reached its maximum strength. The cracking patterns are compatible with those mentioned by other authors [19, 25, 31, 32], with a wide variance which may be explained by the fiber's

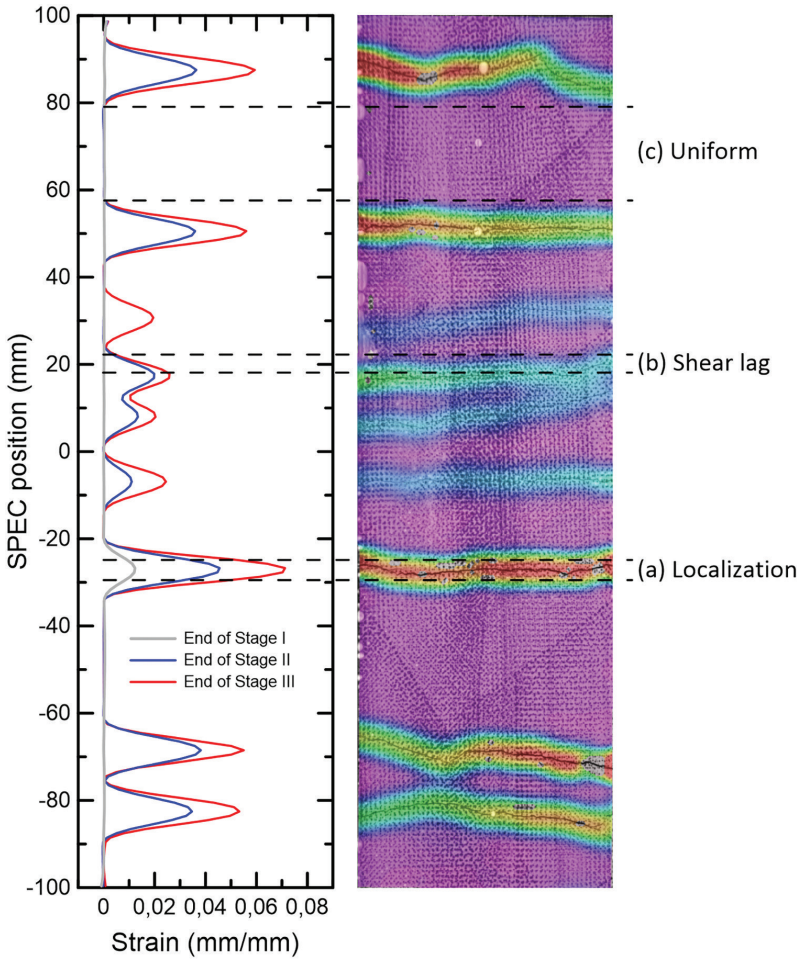

Figure 5: Cracking diagram concerning the stages and the identification of the DIC zones.

Table 4: The DIC composite cracking parameters from tensile tests.

SPECIMEN	DIC CRACK ANALYSIS		
	NUMBER OF CRACKS (unit)	MEAN CRACK WIDTH (µm)	MEAN CRACK SPACING (mm)
SPEC 5	9	288 ± 137	20.0
SPEC 6	9	352 ± 167	20.0
SPEC 7	5	508 ± 75	33.3

morphology and their distribution in the matrix. Compared to SPEC 5 and SPEC 6, SPEC 7 presented the largest crack width and the smallest number of cracks, demonstrating that these parameters are inversely proportional, which is explained by the higher stress concentration in each crack due to its smaller number.

Comparing the strain behaviors acquired by LVDTs and DIC (Figure 6), it can be noticed that the DIC strains appear to be more conservative compared to those described by the LVDTs. TEKIELI *et al*. [57] explain that the LVDTs integrated into the tensile test system can overestimate the strain when specimen slips concerning the clamping wedges. Other possible reasons are the LVDTs misaligns during the axial displacement or the specimen rotation. YAO *et al*. [56] noted that the LVDT displacement is usually higher than the DIC measurements during the multiple cracking stages, while in the linear elastic stage the results are comparable, as possible seen at the zooms in Figure 6. It can be explained by the crack's non-homogeneous strain during its opening, which may influence the computational analysis on quantification of the full-field deformations. Other authors [58, 59] also presented these same strain variances in comparisons between LVDT and DIC measurements. From the known points analysis in both stress-strain curves (at the end of stages I, II, and III), it is possible to observe that these variances represent an approximate ratio of 0.84 (DIC/LVDTs), as summarized in Table 5.

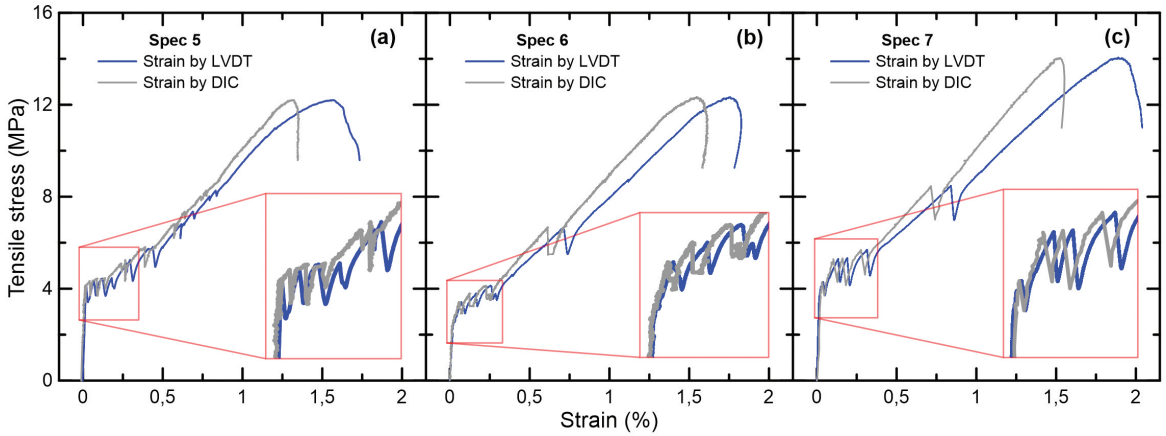

Figure 6: The graphic comparison between LVDTs and DIC strains along same tensile stress: SPEC 5 (a), SPEC 6 (b) and SPEC 7 (c).

Table 5: The comparison between LVDTs and DIC strain measurements form tensile tests.

SPECIMEN	POSITION (end of)	STRESS (MPa)	STRAIN BY LVDTS (%)	STRAIN BY DIC (%)	STRAIN RATIO (DIC/LVDTs)	MEAN STRAIN RATIO
SPEC 5	Stage I	4.2	0.020	0.015	0.77	0.84 ± 0.07
	Stage II	8.3	0.832	0.773	0.93	
	Stage III	12.2	1.567	1.317	0.84	
SPEC 6	Stage I	3.4	0.072	0.056	0.79	0.84 ± 0.04
	Stage II	6.7	0.713	0.614	0.86	
	Stage III	12.3	1.757	1.550	0.88	
SPEC 7	Stage I	4.3	0.040	0.033	0.83	0.83 ± 0.02
	Stage II	8.5	0.840	0.715	0.85	
	Stage III	14.0	1.888	1.527	0.81	

4. CONCLUSIONS

This paper presents valuable information about the tensile behavior of cement-based composites reinforced with sisal fibers in continuous and aligned configuration, comparing direct (LVDTs) and indirect (DIC) methods of strain acquisition. From the direct tensile tests on cementitious composites with 5% fibrous reinforcement per sample volume, the following conclusions could be drawn:

All the continuous fiber-reinforced cement composites presented strain-hardening behavior with strength and strain capacity consistent with the literature, which means the sisal fibers, the used matrix, and the manufacturing protocols provided a high-performance material, potentially useable in the construction industry.

Through the cracking analysis it was possible to associate the material's mechanical behavior with its failure mechanisms, which is crucial for understanding its characteristics of ductility and increased stiffness. It was possible to observe that the stress is not uniformly distributed but locally concentrated in the cracked regions, which leads to the identified zones: Localization, Shear lag, and Uniform.

The strain comparison involving LVDTs and DIC methods showed that the physical measurements can be overvalued when compared to those without physical contact. This variance can be associated with the rigidity of the test system, which may present some misaligning during displacement. In the present work, the DIC measurements represent approximately 84% of LVDTs results, but this ratio can vary depending on the kind of test, the test system integrity, and the DIC setup parameters.

5. ACKNOWLEDGMENTS

The authors acknowledge support from the Brazilian funding agencies CNPq, CAPES, FINEP, and FAPERJ. Felipe Pinheiro Teixeira thanks PROPPG/UENF for the financial support.

6. REFERENCES

[1] ARDANUY, M., CLARAMUNT, J., TOLEDO FILHO, R.D., "Cellulosic fiber reinforced cement-based composites: a review of recent," *Construction and Building Materials*, v. 79, pp. 115–128, 2015. doi: https://doi.org/10.1016/j.conbuildmat.2015.01.035.

[2] SAVASTANO JUNIOR, H., WARDEN, P.G., COUTTS, R.S.P., "Brazilian waste fibres as reinforcement for cement-based composites", *Cement and Concrete Composites*, v. 22, n. 5, pp. 379–384, 2000. doi: http://dx.doi.org/10.1016/S0958-9465(00)00034-2.

[3] TOLÊDO FILHO, R.D., GHAVAMI, K., ENGLAND, G.L., *et al*., "Development of vegetable fibre-mortar composites of improved durability", *Cement and Concrete Composites*, v. 25, n. 2, pp. 185–196, 2003. doi: http://dx.doi.org/10.1016/S0958-9465(02)00018-5.

[4] ANDRADE SILVA, F., MOBASHER, B., TOLEDO FILHO, R.D., "Fatigue behavior of sisal fiber reinforced cement composites", *Materials Science and Engineering A*, v. 527, n. 21–22, pp. 5507–5513, 2010. doi: http://dx.doi.org/10.1016/j.msea.2010.05.007.

[5] SILVA, F.A., TOLEDO FILHO, R.D., MELO FILHO, J.A., *et al*., "Physical and mechanical properties of durable sisal fiber–cement composites", *Construction & Building Materials*, v. 24, n. 5, pp. 777–785, 2010. doi: http://dx.doi.org/10.1016/j.conbuildmat.2009.10.030.

[6] MERTA, I., TSCHEGG, E.K., "Fracture energy of natural fibre reinforced concrete", *Construction & Building Materials*, v. 40, pp. 991–997, 2013. doi: http://dx.doi.org/10.1016/j.conbuildmat.2012.11.060.

[7] HAMZAOUI, R., GUESSASMA, S., MECHERI, B., *et al*., "Microstructure and mechanical performance of modified mortar using hemp fibres and carbon nanotubes", *Materials & Design*, v. 56, pp. 60–68, 2014. doi: http://dx.doi.org/10.1016/j.matdes.2013.10.084.

[8] AGOPYAN, V., SAVASTANO JUNIOR, H., JOHN, V.M., *et al*., "Developments on vegetable fibre-cement based materials in São Paulo, Brazil: an overview", *Cement and Concrete Composites*, v. 27, n. 5, pp. 527–536, 2005. doi: http://dx.doi.org/10.1016/j.cemconcomp.2004.09.004.

[9] RODRÍGUEZ, N.J., YÁÑEZ-LIMÓN, M., GUTIÉRREZ-MICELI, F.A., *et al*., "Assessment of coconut fibre insulation characteristics and its use to modulate temperatures in concrete slabs with the aid of a finite element methodology", *Energy and Building*, v. 43, n. 6, pp. 1264–1272, 2011. doi: http://dx.doi.org/10.1016/j.enbuild.2011.01.005.

[10] GUNASEKARAN, K., ANNADURAI, R., KUMAR, P.S., "A study on some durability properties of coconut shell aggregate concrete", *Materials and Structures*, v. 48, n. 5, pp. 1253–1264, 2015. doi: http://dx.doi.org/10.1617/s11527-013-0230-2.

[11] GUNASEKARAN, K., KUMAR, P.S., LAKSHMIPATHY, M., "Mechanical and bond properties of coconut shell concrete", *Construction & Building Materials*, v. 25, n. 1, pp. 92–98, 2011. doi: http://dx.doi.org/10.1016/j.conbuildmat.2010.06.053.

[12] MERTA, I., MLADENOVIČ, A., TURK, J., *et al*., "Life cycle assessment of natural fibre reinforced cementitious composites", *Key Engineering Materials*, v. 761, pp. 204–209, 2018. doi: http://dx.doi.org/10.4028/www.scientific.net/KEM.761.204.

[13] ERNESTINA ALVES FIDELIS, M., DE ANDRADE SILVA, F., TOLEDO FILHO, R.D., *et al*., "The mechanics of natural jute textile reinforced concrete", In: Brameshuber, W. (ed), *Proceedings of the 11th International Symposium on Ferrocement and 3rd ICTRC International Conference on Textile Reinforced Concrete*, Aachen, pp. 255–266, 7–10 June 2015. https://publications.rwth-aachen.de/record/483483?ln=de, accessed in June, 2022.

[14] EL MESSIRY, M., EL-TARFAWY, S., EL DEEB, R., "Study pultruded Jute fabric effect on the cementitious thin composites mechanical properties with low fiber volume fraction", *Alexandria Engineering Journal*, v. 56, n. 4, pp. 415–421, 2017. doi: http://dx.doi.org/10.1016/j.aej.2017.05.026.

[15] FIDELIS, M.E.A., TOLEDO FILHO, R.D., SILVA, F.A., *et al*., "The effect of accelerated aging on the interface of jute textile reinforced concrete", *Cement and Concrete Composites*, v. 74, pp. 7–15, 2016. doi: http://dx.doi.org/10.1016/j.cemconcomp.2016.09.002.

[16] ZUKOWSKI, B., DE ANDRADE SILVA, F., TOLEDO FILHO, R.D., "Design of strain hardening cement-based composites with alkali treated natural curauá fiber", *Cement and Concrete Composites*, v. 89, pp. 150–159, 2018. doi: http://dx.doi.org/10.1016/j.cemconcomp.2018.03.006.

[17] SOLTAN, D.G., DAS NEVES, P., OLVERA, A., *et al*., "Introducing a curauá fiber reinforced cement-based composite with strain-hardening behavior", *Industrial Crops and Products*, v. 103, pp. 1–12, 2017. doi: http://dx.doi.org/10.1016/j.indcrop.2017.03.016.

[18] HWANG, C.L., TRAN, V.A., HONG, J.W., *et al*., "Effects of short coconut fiber on the mechanical properties, plastic cracking behavior, and impact resistance of cementitious composites", *Construction & Building Materials*, v. 127, pp. 984–992, 2016. doi: http://dx.doi.org/10.1016/j.conbuildmat.2016.09.118.

[19] SOUZA, L.O., SOUZA, L.M.S., SILVA, F.A., "Mechanics of natural curauá textile-reinforced concrete", *Magazine of Concrete Research*, v. 73, n. 3, pp. 135–146, 2021. doi: http://dx.doi.org/10.1680/jmacr.18.00473.

[20] MELO FILHO, J.A., SILVA, F.A., TOLEDO FILHO, R.D., "Degradation kinetics and aging mechanisms on sisal fiber cement composite systems", *Cement and Concrete Composites*, v. 40, pp. 30–39, 2013. doi: http://dx.doi.org/10.1016/j.cemconcomp.2013.04.003.

[21] D'ALMEIDA, A.L.S., MELO FILHO, J.A., TOLEDO FILHO, R.D., "Use of curaua fibers as reinforcement in cement composites", *Chemical Engineering Transactions*, v. 17, pp. 1717–1722, 2009. doi: http://dx.doi.org/10.3303/CET0917287.

[22] WU, M., JOHANNESSON, B., GEIKER, M., "A review: self-healing in cementitious materials and engineered cementitious composite as a self-healing material", *Construction & Building Materials*, v. 28, n. 1, pp. 571–583, 2012. doi: http://dx.doi.org/10.1016/j.conbuildmat.2011.08.086.

[23] WEI, J., GENCTURK, B., "Degradation of natural fiber in cement composites containing diatomaceous earth", *Journal of Materials in Civil Engineering*, v. 30, n. 11, pp. 1–17, 2018. doi: http://dx.doi.org/10.1061/(ASCE)MT.1943-5533.0002486.

[24] FERREIRA, S.R., LIMA, P.R.L., SILVA, F.A., *et al*., "Influência de ciclos molhagem-secagem em fibras de sisal sobre a aderência com matrizes de cimento Portland", *Matéria (Rio de Janeiro)*, v. 17, n. 2, pp. 1024–1034, 2012. doi: http://dx.doi.org/10.1590/S1517-70762012000200008.

[25] SILVA JUNIOR, I.B., SOUZA, L.M.S., SILVA, F.A., "Creep of pre-cracked sisal fiber reinforced cement based composites", *Construction & Building Materials*, v. 293, pp. 123511, 2021. doi: http://dx.doi.org/10.1016/j.conbuildmat.2021.123511.

[26] CLARAMUNT, J., ARDANUY, M., GARCÍA-HORTAL, J.A., *et al*., "The hornification of vegetable fibers to improve the durability of cement mortar composites", *Cement and Concrete Composites*, v. 33, n. 5, pp. 586–595, 2011. doi: http://dx.doi.org/10.1016/j.cemconcomp.2011.03.003.

[27] FERREIRA, S.R., LIMA, P.R.L., SILVA, F.A., *et al*., "Influência de ciclos molhagem-secagem em fibras de sisal sobre a aderência com matrizes de cimento Portland", *Revista de Matemáticas*, v. 17, pp. 1024–1034, 2012. doi: http://dx.doi.org/10.1590/S1517-70762012000200008.

[28] FERREIRA, S.R., SILVA, F.D.A., LIMA, P.R.L., *et al*., "Effect of fiber treatments on the sisal fiber properties and fiber-matrix bond in cement based systems", *Construction & Building Materials*, v. 101, pp. 730–740, 2015. doi: http://dx.doi.org/10.1016/j.conbuildmat.2015.10.120.

[29] WEI, J., MEYER, C., "Sisal fiber-reinforced cement composite with Portland cement substitution by a combination of metakaolin and nanoclay", *Journal of Materials Science*, v. 49, n. 21, pp. 7604–7619, 2014. doi: http://dx.doi.org/10.1007/s10853-014-8469-8.

[30] CASTOLDI, R.S., DE SOUZA, L.M.S., DE ANDRADE SILVA, F., "Comparative study on the mechanical behavior and durability of polypropylene and sisal fiber reinforced concretes", *Construction & Building Materials*, v. 211, pp. 617–628, 2019. doi: http://dx.doi.org/10.1016/j.conbuildmat.2019.03.282.

[31] SILVA, F.A., MOBASHER, B., FILHO, R.D.T., "Cracking mechanisms in durable sisal fiber reinforced cement composites", *Cement and Concrete Composites*, v. 31, n. 10, pp. 721–730, 2009. doi: http://dx.doi.org/10.1016/j.cemconcomp.2009.07.004.

[32] TEIXEIRA, F.P., SILVA, F.A., "On the use of natural curauá reinforced cement based composites for structural applications", *Cement and Concrete Composites*, v. 114, pp. 103775, 2020. doi: http://dx.doi.org/10.1016/j.cemconcomp.2020.103775.

[33] HAGGER, J., WILL, N., ALDEA, C., *et al*., "Applications of textile reinforced concrete", In: Brameshuber, W. (ed), Textile Reinforced Concrete – State-of-the-Art Report of RILEM TC 201-TRC, Paris, FR, RILEM Publications SARL, pp. 237–270, 2006.

[34] FERREIRA, S.R., SILVA, F.A., LIMA, P.R.L., *et al*., "Effect of hornification on the structure, tensile behavior and fiber matrix bond of sisal, jute and curauá fiber cement based composite systems", *Construction & Building Materials*, v. 139, pp. 551–561, 2017. doi: http://dx.doi.org/10.1016/j.conbuildmat.2016.10.004.

[35] SINGH, S., SHUKLA, A., BROWN, R., "Pullout behavior of polypropylene fibers from cementitious matrix", *Cement and Concrete Research*, v. 34, n. 10, pp. 1919–1925, 2004. doi: http://dx.doi.org/10.1016/j.cemconres.2004.02.014.

[36] ASPRONE, D., DURANTE, M., PROTA, A., *et al*., "Potential of structural pozzolanic matrix-hemp fiber grid composites", *Construction & Building Materials*, v. 25, n. 6, pp. 2867–2874, 2011. doi: http://dx.doi.org/10.1016/j.conbuildmat.2010.12.046.

[37] MAAGE, M., "Interaction between steel fibers and cement based matrixes", *Matériaux et Construction*, v. 10, pp. 297–301, 1977. doi: http://dx.doi.org/10.1007/BF02478831.

[38] CHAN, Y., LI, V.C., "Effects of transition zone densification on fiber/cement paste bond strength Improvement", *Advanced Cement Based Materials*, v. 5, n. 1, pp. 8–17, 1997. doi: http://dx.doi.org/10.1016/S1065-7355(97)90010-9.

[39] SHANNAG, M.J., BRINCKER, R., HANSEN, W., "Pullout behavior of steel fibers from cement-based composites", *Cement and Concrete Research*, v. 27, n. 6, pp. 925–936, 1997. doi:http://dx.doi.org/10.1016/S0008-8846(97)00061-6.

[40] LI, V., STANG, H., "Interface property characterization and strengthening mechanisms in fiber reinforced cement based composites", *Advanced Cement Based Materials*, v. 6, n. 1, pp. 1–20, 1997. doi: http://dx.doi.org/10.1016/S1065-7355(97)90001-8.

[41] GRAY, R.J., JOHNSTON, C.D., "The influence of fibre-matrix interfacial bond strength on the mechanical properties of steel fibre reinforced mortars", *International Journal of Cement Composites and Lightweight Concrete*, v. 9, n. 1, pp. 43–55, 1987. doi: http://dx.doi.org/10.1016/0262-5075(87)90036-4.

[42] TEIXEIRA, F.P., LIMA, V.N., MOUTINHO, D.J.C., *et al*., "Mechanical properties and fractography of cement-based composites reinforced by natural piassava and jute fibers", *Cerâmica*, v. 68, n. 385, pp. 60–66, 2022. doi: http://dx.doi.org/10.1590/0366-69132022683853174.

[43] TEIXEIRA, F.P., CARDOSO, D.C.T., DE ANDRADE SILVA, F., "On the shear behavior of natural curauá fabric reinforced cement-based composite systems", *Engineering Structures*, v. 246, pp. 113054, 2021. doi: http://dx.doi.org/10.1016/j.engstruct.2021.113054.

[44] LI, V.C., STANG, H., KRENCHEL, H., "Micromechanics of crack bridging in fibre-reinforced concrete", *Materials and Structures*, v. 26, n. 8, pp. 486–494, 1993. doi: http://dx.doi.org/10.1007/BF02472808.

[45] LÖFGREN, I., *Fibre-reinforced Concrete for Industrial Construction – a fracture mechanics approach to material testing and structural analysis*, Göteborg, Sweden, Chalmers University of Technology, 2005.

[46] BENTUR, A., MINDESS, S., *Fibre reinforced cementitious composites*, 2 ed., New York, Taylor & Francis, 2007.

[47] YAO, Y., SILVA, F.A., BUTLER, M., *et al*., "Tension stiffening in textile-reinforced concrete under high speed tensile loads", *Cement and Concrete Composites*, v. 64, pp. 49–61, 2015. doi: http://dx.doi.org/10.1016/j.cemconcomp.2015.07.009.

[48] MOBASHER, B., PAHILAJANI, J., PELED, A., "Analytical simulation of tensile response of fabric reinforced cement based composites", *Cement and Concrete Composites*, v. 28, n. 1, pp. 77–89, 2006. doi: http://dx.doi.org/10.1016/j.cemconcomp.2005.06.007.

[49] SILVA, F.A., CHAWLA, N., DE TOLEDO FILHO, R.D., "An experimental investigation of the fatigue behavior of sisal fibers", *Materials Science and Engineering A*, v. 516, n. 1–2, pp. 90–95, 2009. doi: http://dx.doi.org/10.1016/j.msea.2009.03.026.

[50] TEIXEIRA, F.P., GOMES, O.F.M., SILVA, F.A., "Degradation mechanisms of curaua, hemp, and sisal fibers exposed to elevated temperatures", *BioResources*, v. 14, n. 1, pp. 1494–1511, 2019. doi: http://dx.doi.org/10.15376/biores.14.1.1494-1511.

[51] AZWA, Z.N., YOUSIF, B.F., MANALO, A.C., *et al*., "A review on the degradability of polymeric composites based on natural fibres", *Materials & Design*, v. 47, pp. 424–442, 2013. doi: http://dx.doi.org/10.1016/j.matdes.2012.11.025.

[52] YAN, L., KASAL, B., HUANG, L., "A review of recent research on the use of cellulosic fibres, their fibre fabric reinforced cementitious, geo-polymer and polymer composites in civil engineering", *Composites. Part B, Engineering*, v. 92, pp. 94–132, 2016. doi: http://dx.doi.org/10.1016/j.compositesb.2016.02.002.

[53] ASSOCIAÇÃO BRASILEIRA DE NORMAS TÉCNICAS, *ABNT NBR 16697 Cimento Portland – Requisitos*, Rio de Janeiro, ABNT, 2018.

[54] BRUCK, H.A., MCNEILL, S.R., SUTTON, M.A., *et al*., "Digital image correlation using Newton-Raphson method of partial differential correction", *Experimental Mechanics*, v. 29, n. 3, pp. 261–267, 1989. doi: http://dx.doi.org/10.1007/BF02321405.

[55] SUTTON, M., WOLTERS, W., PETERS, W., *et al*., "Determination of displacements using an improved digital correlation method", *Image and Vision Computing*, v. 1, n. 3, pp. 133–139, 1983. doi: http://dx.doi.org/10.1016/0262-8856(83)90064-1.

[56] YAO, Y., SILVA, F.A., BUTLER, M., *et al*., "Tension stiffening in textile-reinforced concrete under high speed tensile loads", *Cement and Concrete Composites*, v. 64, pp. 49–61, 2015. doi: http://dx.doi.org/10.1016/j.cemconcomp.2015.07.009.

[57] TEKIELI, M., DE SANTIS, S., DE FELICE, G., *et al*., "Application of digital image correlation to composite reinforcements testing", *Composite Structures*, v. 160, pp. 670–688, 2017. doi: http://dx.doi.org/10.1016/j.compstruct.2016.10.096.

[58] D'ANTINO, T., PAPANICOLAOU, C.C., Comparison between different tensile test set-ups for the mechanical characterization of inorganic-matrix composites", *Construction & Building Materials*, v. 171, pp. 140–151, 2018. doi: http://dx.doi.org/10.1016/j.conbuildmat.2018.03.041.

[59] LOPES, J., STEFANIAK, D., REIS, L., *et al*., "Single lap shear stress in hybrid CFRP/steel composites", *Procedia Structural Integrity*, v. 1, pp. 58–65, 2016. doi: http://dx.doi.org/10.1016/j.prostr.2016.02.009.